Developments in the Built Environment 28 (2026) 101070



Contents lists available at ScienceDirect

Developments in the Built Environment

journal homepage: www.sciencedirect.com/journal/developments-in-the-built-environment



Window shading and materiality for psychophysiological stress in hospital waiting areas: a Spatial Frequency perspective through amplitude spectrum slopes in Virtual Reality

Mirna Zordan *, Zixian Lei, Jiakun Pei

School of Design, Southern University of Science and Technology, 3F Building C1, Nanshan iPark, No.1001 XueYuan Avenue, Nanshan, Shenzhen, 518055, China

ARTICLE INFO

Keywords:
Hospital waiting areas
Psychophysiological stress
Spatial frequency
Amplitude spectrum slope
Materiality
Window shading

ABSTRACT

Indoor Environmental Quality (IEQ) can influence psychophysiological stress in hospital waiting areas; however, specific visual features warrant further investigation. We introduce amplitude spectrum slope ($-\alpha$) as an image-based metric that characterizes Spatial Frequency in scene images and participants' recorded views. We conducted a VR experiment where 47 healthy young adults viewed conditions combining open/closed blinds and biophilic/artificial materiality. Outcomes included STAI-S, EEG-derived FAA, HRV-derived RMSSD, and preference ratings. Open blinds and biophilic materiality showed smaller STAI-S changes (b = −0.301, −0.444) and larger RMSSD changes (b = 2.877, 2.665 ms). In separate mixed models adjusted for age, gender, and STAI-T, each 0.1 decrease in personal α towards 1 (range: 1–2) was associated with lower STAI-S (−0.361), and higher RMSSD (+2.296 ms) and FAA (+0.092). Our findings support open blinds and biophilic materiality in fostering reduced stress in healthcare environments, while α provided a spectral measure for visual IEQ assessment.

1. Introduction

Stress is widely recognized as an important public health concern (Stress: The Health Epidemic of, 2016). Psychological and physiological stress can easily arise when environmental quality fails to meet individual needs, such as poor housing quality, overcrowded spaces, and insufficient natural light (Evans, 1984, 2003). Conversely, supportive environments have the potential to alleviate stress. As most people spend 80-90% of their time indoors, Indoor Environmental Quality (IEQ) has emerged as a key determinant of stress levels (Zhang et al., 2023; Manu et al., 2024; Guo et al., 2024; Evans and McCoy, 1998).

Hospitals are particularly relevant in this regard because patients and visitors often experience heightened vulnerability, uncertainty, and emotional tension during medical visits (Mourshed and Zhao, 2012; Ulrich et al., 2008; Wu et al., 2023). Poor IEQ in hospital settings can lead to environmental discomfort, amplifying psychological and physiological stress (Nimlyat and Kandar, 2015; Lundberg et al., 2024). Therefore, many studies have begun exploring how IEQ affects stress in healthcare areas. For instance, thermally comfortable environments support mood stability and recovery (Khodakarami and Nasrollahi, 2012; Rus et al., 2022). Among acoustic factors, noise is a major source of patient dissatisfaction, linked to increased stress and weakened immune response, while natural sounds can alleviate stress (Zhou et al., 2020). Regarding air quality, it strongly influences environmental satisfaction and significantly affects individuals' long-term stress (Wu et al., 2023; Zhang et al., 2020). Moreover, for visual factors, elements such as indoor greenery, nature views, biophilic decorations, and adequate lighting have been associated with reduced stress and shorter hospital stays (Beukeboom et al., 2012; Ohta et al., 2008).

Among healthcare spaces, hospital waiting areas warrant particular attention. Patients and visitors may spend extended periods in these spaces while awaiting consultations, procedures, or medical information, and such waiting experiences may be accompanied by uncertainty and anticipatory stress (Lundberg et al., 2024). Previous evidence suggests that waiting times in hospital settings can be substantial, with reported averages ranging from 55.27 to 71.28 min in waiting areas (Dansky and Miles, 1997). Despite its importance, limited evidence is available on how the IEQ of hospital waiting areas relates to stress among patients and visitors, suggesting the need for more targeted empirical investigations.

* Corresponding author. 3F, Building C1, Nanshan iPark, No.1001 XueYuan Avenue, Nanshan, 518055, Shenzhen, China.
E-mail addresses: mzordan@sustech.edu.cn (M. Zordan), lzxlook@gmail.com (Z. Lei), 12531633@mail.sustech.edu.cn (J. Pei).

https://doi.org/10.1016/j.dibe.2026.101070
Received 16 July 2026; Received in revised form 27 September 2026; Accepted 8 October 2026
Available online 9 October 2026
2666-1659/© 2026 The Authors. Published by Elsevier Ltd. This is an open access article under the CC BY-NC-ND license (http://creativecommons.org/licenses/by-nc-nd/4.0/).

1.1. Vision and indoor environment

In the multisensory experience of built environments, visual perception enables the recognition of elements such as spatial configuration, scale, light and shadow, color, and materiality (Gibson, 2014; McGee et al., 2019), and is generally considered the dominant mode of perception (Posner et al., 1976). Beyond its role in perceiving the built environment, vision also significantly contributes to the evaluation of environmental quality, with visual factors becoming essential components in IEQ assessment. These visual factors can be broadly categorized into lighting-related and non-lighting-related elements. Lighting-related visual factors primarily include photometric variables, glare, and light color temperature (Mott et al., 2013; Garciai and Wierwille, 1985; Ochoa and Capeluto, 2006). Non-lighting-related visual factors encompass various aspects of the interior environment, such as surface textures, spatial layout, decorative features, color schemes, window views, and biophilic elements (Wang et al., 2021). In healthcare waiting areas, these visual factors may be particularly relevant because users often remain in the space for extended periods while experiencing uncertainty or anticipatory tension. This study examines the effects of two visual factors, window shading and materiality, on stress-related psychological and physiological responses in simulated hospital waiting area environments.

1.1.1. The impact of window shading

Windows provide natural light and outdoor views, acting as a source of visual stimuli that may elicit physiological and psychological responses (Chang and Chen, 2005). For example, waiting areas with larger or multiple windows that provide more natural light and outside views tend to create a more open and inviting atmosphere, enhancing neural and visual stimulation, and contributing to lower stress levels, anxiety levels, and better recovery outcomes (Emami et al., 2024; Jiang et al., 2017). Natural landscape views are typically linked to higher environmental satisfaction and lower stress levels, while views of neighboring buildings or the absence of windows are often associated with poorer satisfaction (Chang and Chen, 2005).

However, the study of windows should extend beyond the simple dichotomy of “windows” versus “no windows”. The specific design of window shading, such as blinds, curtains, or dimming glass, also influences how windows deliver visual stimuli. In a recent study, an image-based nationwide online survey was conducted in the United States with 250 patients who had recently received hospital care. Results revealed that different shading configurations, including blind positions and window tint, varied patients' perceptions. The study found that opening blinds in inpatient rooms significantly improved patients' satisfaction with the room, hospital, and the quality of care, while also supporting their mood and reducing stress (Jafarifiroozabadi et al., 2022). Additionally, a study observing 11 cardiac ICU patients for 22 days found that anxiety and depression scores, as well as analgesic use, were significantly reduced when blinds were open for more than 50% of the day. This suggests that the blind openness can function as a non-pharmacological intervention to improve patient status (Jafarifiroozabadi, 2025). However, image-based assessments may introduce cognitive bias, and many of these studies are limited to self-reported data on patient experience, satisfaction, and perceived quality of the hospital environment. Furthermore, there is a general lack of empirical research combining psychological and physiological data to validate the impact of window shading on individuals’ stress-related responses in hospital waiting areas.

1.1.2. The impact of materiality

Materiality is another important non-lighting visual factor in interior environments. In this study, materiality is considered in terms of its visual expression. Specifically, biophilic materiality in this study refers to finishes that visually evoke natural characteristics, such as wood and stone, whereas artificial materiality refers to finishes with more synthetic or non-natural visual characteristics. The selection of wood and stone finishes was informed by established biophilic design frameworks, which identify natural materials as an attribute of biophilic design (Kellert et al., 2008; Kellert and Calabrese, 2015). Incorporating natural elements into hospital waiting areas, as opposed to relying solely on artificial materiality, has often been linked to reduced stress and anxiety (McGee et al., 2019). Features such as strategically placed plants, including real or artificial plant decorations, and nature-inspired artwork have been found to significantly reduce patients' stress levels (Emami et al., 2024; Hall and Knuth, 2019). Additionally, the use of natural materials, such as wood, in the decoration of interior environments, including walls, ceilings, and furniture, has been found to positively influence individuals’ physiological responses, emotional states, and cognitive performance, both through direct visual exposure and in Virtual Reality (VR) settings (Emami et al., 2024; Li et al., 2021; Lipovac and Burnard, 2021; Du et al., 2025). However, most of these studies have limitations, such as an over-reliance on self-reported data, raising concerns about subjectivity and measurement validity.

1.2. Visual perception, visual complexity, and spatial frequency

In the study of visual perception, contemporary researchers in psychophysics and psychometrics have proposed methods to quantify subjective experiences and establish mathematical relationships between visual perception and its corresponding physical components (Fechner, 1948; Teghtsoonian, 1975). Visual perception is fundamentally dependent on visual stimuli, which typically exhibit varying degrees of visual complexity and may evolve over time (Hochberg, 1957). Visual complexity has become an important factor in understanding human perceptions in built environments, with its role in human responses to different environmental contexts widely recognized (Donderi, 2006; Lee and Ostwald, 2023; Ma et al., 2021). This concept is also integral to design practice. Key elements contributing to the perception of visual complexity include the number of objects in a scene, the degree of disarray, openness, symmetry, organization, and color diversity (Berlyne, 1960; Olivia et al., 2004).

To characterize why one visual scene may be perceived as more complex than another, researchers have developed several analytical frameworks of visual complexity, such as fractal (Jacquin, 1992), fuzzy (Cardaci et al., 2009), and information theory (Rigau et al., 2005). Among these, Spatial Frequency (SF) analysis provides an image-based approach for describing how visual information is distributed across spatial scales (Durmus, 2020; Kawamoto, 2002). Studies have shown that SF characteristics are related to the perception of visual complexity (Cavalcante et al., 2014), with interactions between visual complexity and SF processing also reported (Gong et al., 2023).

SF can be categorized into Low Spatial Frequency (LSF) and High Spatial Frequency (HSF). LSF conveys coarse, global information about the scene (e.g., the overall outline), is processed quickly, and plays a key role in overall perception. In contrast, HSF conveys fine details and explicit boundary information, processed through different neural pathways, and is crucial for local information processing and the presentation of detailed features, which are typical features of complex scenes. Research indicates that both high- and low-frequency components contribute critically to accurate identification of complex visual targets (Bullier, 2001).

SF analysis characterizes how image information is distributed across spatial scales, helping to explain how different frequency components contribute to the perception of scene details and overall structure. Rather than treating SF as a direct causal mechanism, this study uses SF characteristics as quantitative descriptors of visual scene structure. This approach provides a quantitative framework for characterizing image properties associated with visual complexity. When combined with psychological and physiological measurements, SF descriptors may help examine whether visual scene structure is associated with stress-related responses in simulated hospital waiting areas.

1.2.1. Spatial frequency and $1/f^{\alpha}$ amplitude spectrum

The amplitude spectrum slope quantifies the distribution of SF information in an image. Many images exhibit a power-law distribution of amplitude across frequencies, commonly approximated by a $1/f^{\alpha}$ function. The function is formulated as follows:

$$A(f) \propto f^{-\alpha} \tag{1}$$

In this context, amplitude $A(f)$ is averaged across all directions, f represents the SF, and $-\alpha$ is the slope in log-log coordinates (Bex and Makous, 2002), which reflects the balance between low and high SF content (Isherwood et al., 2017). The amplitude spectrum slope ($-\alpha$) varies between images, with typical α values ranging from 0.7 to 1.5 in achromatic images, and images with more natural spectra often exhibit α values close to 1 and are associated with lower visual discomfort (Bex and Makous, 2002; Field, 1987; Juricevic et al., 2010a; Tolhurst et al., 1992). In this sense, α is derived from the visual content of scene images and describes their SF structure rather than serving as a direct indicator of stress. However, whether α values are associated with stress-related responses in hospital waiting areas remains unclear.

1.3. Research objectives and contributions

Although previous research has highlighted the impact of visual factors on stress and well-being in healthcare environments, several issues remain underexplored. In particular, limited experimental evidence is available on how materiality (artificial vs. biophilic) and window shading (open vs. closed blinds) are associated with psychological and physiological stress-related responses in hospital waiting areas. In addition, although SF metrics such as the amplitude spectrum slope ($-\alpha$) can describe image properties related to visual complexity, their relevance to stress-related responses in hospital waiting areas remains insufficiently examined.

Therefore, this study uses VR-based environmental simulation to examine how materiality and window shading are associated with psychological and physiological stress-related responses in simulated hospital waiting areas. It further uses α as an image-based descriptor to characterize the spectral structure of the simulated scenes and participants' recorded views, and examines associations between personal α and stress-related responses across the experimental conditions.

The study makes two contributions: experimental evidence on stress-related responses to waiting-area design conditions, and evidence supporting the use of personal α as an image-based spectral descriptor of visual scene structure for IEQ assessment. Together, these findings provide a quantitative reference for evaluating window shading and materiality in hospital waiting-area design.

2. Methods

2.1. Participants

An a priori sample size estimation was conducted using G*Power 3.1 (Faul et al., 2009). Because the study used a within-subject design with four experimental conditions, the planning estimate was based on the closest repeated-measures F-test framework, with one group and four repeated measurements. A conventional medium effect size of f = 0.25 was adopted following Cohen's benchmark (Cohen, 2013), with an alpha level of 0.05 and a desired power of 0.80. The minimum required sample size was estimated as 24 participants. A total of 47 healthy adults were recruited, exceeding the a priori estimate.

Prior to participation, all participants completed a screening battery to ensure eligibility and to minimize confounding variables. Inclusion criteria required participants to be free of psychiatric or neurological disorders and possess normal or corrected-to-normal vision. Exclusion criteria included color-vision deficiencies, a history of severe photosensitivity, self-reported susceptibility to motion sickness or VR-induced discomfort, prior involvement in similar biofeedback experiments, or professional engagement in healthcare spatial design. Participants were instructed to obtain a full night's sleep and refrain from caffeine for at least 12 h before the experiment.

Participant sociodemographic data are summarized in Table 1. Participants voluntarily enrolled and received compensation for their participation. The study protocol was designed in accordance with The Code of Ethics of the World Medical Association (Declaration of Helsinki) for experiments involving humans, it is in line with the Recommendations for the Conduct, Reporting, Editing and Publication of Scholarly Work in Medical Journals, and was approved by the Institutional Review Board of the corresponding institution (2025PES115).

2.2. Experimental environment setting

To minimize the interference of extraneous variables, a validated three-dimensional VR representation was adopted to simulate a hospital waiting area environment (Higuera-Trujillo et al., 2017). Two visual factors were manipulated, each at two levels: window shading (closed vs. open blinds) and materiality (biophilic vs. artificial). These two factors were treated as visual design conditions, each comprising multiple visual attributes. The study examined participants' responses to the open-versus closed-blind conditions and to the two material palettes as a whole, as implemented in the VR environments. In particular, the manipulation of window shading could alter daylight availability, visibility of the outdoor view, perceived openness, luminance distribution, and visual contrast, whereas the manipulation of materiality could alter surface texture, color, and perceived naturalness. Layouts were drafted in AutoCAD 2020, and the architectural models were constructed in Rhinoceros 7. The same spatial layout, furniture arrangement, camera position, and viewing height were maintained across all four conditions. A fixed indoor artificial lighting configuration and a consistent daylight environment were maintained across all virtual conditions, with exposure and rendering settings held constant to minimize potential lighting-related confounding effects. A seated eye height of 770 mm (measured from the seat surface) was adopted based on the ISO 7250-2 anthropometric database (ISO, 2024). The outside view comprised three layers: ground plane, urban or natural landscape, and sky, following guidelines from EN 17037 (EN 17037, 2018) and CIBSE Lighting Guide 10: Daylighting (CIBSE, 2014). High-resolution, 360° isometric panoramas (12,240 × 6120 pixels) were rendered in Blender and imported into an HTC Vive Focus 3 headset via Unity and Vive Stream. Each condition was presented using the same pre-rendered panoramic image for all participants; actual outdoor weather during data collection therefore did not alter the visual stimuli. Four experimental conditions were defined (see Fig. 1).

- Condition A (Open Blinds + Biophilic Materiality): Open blinds with full external views; interior finishes in wood and stone.
- Condition B (Open Blinds + Artificial Materiality): Open blinds with full external views; interior finishes in concrete and ceramic tiles.
- Condition C (Closed Blinds + Biophilic Materiality): Fully closed blinds with limited natural light; interior finishes in wood and stone.
- Condition D (Closed Blinds + Artificial Materiality): Fully closed blinds with limited natural light; interior finishes in concrete and ceramic tiles.

Table 1
Demographic information of study participants.

Variable	Attribute	Number	Percent
Gender	Male	26	55.32%
	Female	21	44.68%
Age	Mean (Std. Dev)	24.79 (±2.45)	-
Participant status	Student	40	85.11%
	Staff	7	14.89%

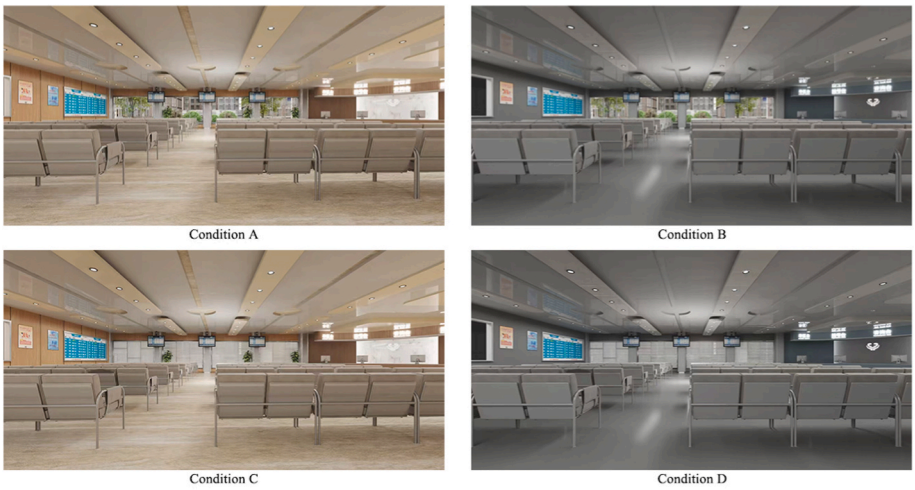


Fig. 1. VR condition scenarios: (A) Open Blinds + Biophilic Materiality; (B) Open Blinds + Artificial Materiality; (C) Closed Blinds + Biophilic Materiality; (D) Closed Blinds + Artificial Materiality.

Following the image-based pixel-ratio principle used in previous visual environmental research (Li et al., 2015; Seiferling et al., 2017), the image coverage of the material manipulation was calculated by dividing the number of pixels corresponding to the surfaces whose finishes were changed between the biophilic and artificial conditions by the total number of pixels in the rendered panorama used for VR presentation. These surfaces occupied approximately 25% of the total pixel area of the analyzed panorama.

2.3. Experimental procedure

A 2×2 within-subjects experimental design was conducted to examine the effects of two visual design conditions, window shading and materiality, on participants' stress-related psychological and physiological responses in VR-simulated hospital waiting area environments. A Latin Square Design was employed to counterbalance the sequence of the four conditions and control for order and position effects.

Each experimental session lasted approximately 65 min. To reduce expectation bias, recruitment materials provided only a minimal description of the study and did not disclose its specific research objectives. Participants signed informed consent and were informed about the experimental procedures, then completed the 20-item State-Trait Anxiety Inventory-Trait (STAI-T) to assess baseline trait stress. This was followed by a preparation period, during which participants were fitted with physiological sensors: the Emotiv Epoc X headset for Electroencephalography (EEG) recording and the EryLife Watch for photoplethysmography (PPG) recording, from which Heart Rate Variability (HRV) indices were subsequently derived. All participants wore the wristband on their non-dominant hand. Next, participants completed the 6-item State-Trait Anxiety Inventory-State (STAI-S) to establish a pre-exposure psychological baseline. Subsequently, participants donned the HTC Vive Focus 3 headset to engage with the VR conditions. An overview of the experimental equipment setup is illustrated in Fig. 2.

At the start of each condition, participants were exposed to a blank virtual scene for 1 min to obtain a condition-specific physiological baseline for EEG and PPG signals. This duration was considered feasible for extracting short EEG segments for spectral analysis, as frontal EEG asymmetry studies commonly estimate alpha asymmetry from multiple short EEG segments or 1-min segments (Towers and Allen, 2009). For PPG-derived HRV, the 1-min baseline was considered acceptable for ultra-short RMSSD estimation based on previous validation studies (Munoz et al., 2015; Esco and Flatt, 2014). Participants were then guided using a standardized neutral instruction to imagine themselves sitting alone in a quiet hospital waiting area, awaiting their turn for a routine consultation, and to observe their surroundings attentively. No information about disease type, diagnosis, prognosis, or possible



Fig. 2. Overview of the experimental equipment setup.

medical outcomes was provided. This was followed by a 3-min exposure to the designated virtual waiting area condition. The 3-min exposure duration was selected based on a previous VR-based built-environment study using 3-min viewing periods for EEG recording (Kim, 2025). It also provided a recording window for calculating RMSSD, as previous studies have supported the use of short-duration recordings for RMSSD estimation (Munoz et al., 2015; Esco and Flatt, 2014). Afterward, the HTC Vive Focus 3 headset was removed, and participants completed the second administration of the 6-item STAI-S.

A 5-min rest period ensued before the next condition to reduce fatigue and potential carryover effects, consistent with a previous VR-based psychophysiological study using 5-min rest periods between conditions (Kim, 2025). Because a full return to the initial baseline could not be assumed, each condition included a new pre-exposure STAI-S assessment and a new 1-min blank-scene physiological baseline. Each of the remaining three conditions followed the same cycle: participants completed a 6-item STAI-S to establish a new baseline, followed by 1 min of a blank virtual scene and 3 min of the waiting area condition, concluding with a post-exposure 6-item STAI-S assessment and a subsequent 5-min rest. During each VR exposure, participants were instructed to observe the surrounding environment freely while remaining silent. After all sessions, physiological sensors were removed, and participants completed a post-experiment questionnaire.

All sessions were conducted in the same laboratory room to minimize variation in laboratory environmental conditions. The room was illuminated exclusively by artificial lighting, with the lighting configuration kept unchanged across sessions. The air-conditioning temperature setpoint was maintained at 24 °C throughout testing. The room configuration, equipment placement, settings, ventilation mode, and experimenter instructions were kept constant across participants and conditions. An overview of the experimental procedure is shown in Fig. 3.

2.4. Measurement methods

2.4.1. Psychological measurement

The State-Trait Anxiety Inventory (STAI) is a widely used instrument for assessing stress levels. The STAI-T consists of 20 items and measures relatively stable trait anxiety, whereas the STAI-S assesses temporary state anxiety (Spielberger et al., 1971). In this study, the full 20-item STAI-T was administered at the beginning of the experiment, while a validated 6-item short form of the STAI-S was administered before and after each experimental condition (Marteau and Bekker, 1992). The STAI-S and STAI-T consist of positively and negatively worded items, rated on a four-point Likert scale ranging from 1 (“not at all”) to 4 (“very much so”) (Appendix A). Positive items were reverse-scored, and negative items were scored directly. Mean scores were computed to represent situational stress levels, with higher scores indicating higher stress levels. A post-experiment questionnaire was administered to collect participant demographic information and to assess their preferences for each condition using a five-point Likert scale (Appendix B).

2.4.2. Physiological measurements

In this study, EEG and PPG-derived HRV were utilized as physiological measures related to stress responses. EEG signals were recorded using the Emotiv Epoc X headset (EMOTIV Inc., USA), which includes 14 channels and is validated for capturing brain activity (Williams et al., 2020). EEG signals were sampled at 256 Hz using the Emotiv PRO software and were processed using MATLAB R2023a and the EEGLAB toolbox (Delorme and Makeig, 2004). After importing the data and defining electrode locations, a bandpass filter (1-40 Hz) was applied to the EEG signals. Independent Component Analysis (ICA) was performed to remove artifacts, including eye blinks, head movements, and muscle artifacts. Cleaned EEG data were segmented into 2-s epochs with a 50% overlap. Noisy segments and epochs exceeding ±100 μV were excluded. Condition-level EEG recordings were excluded from the FAA analysis if

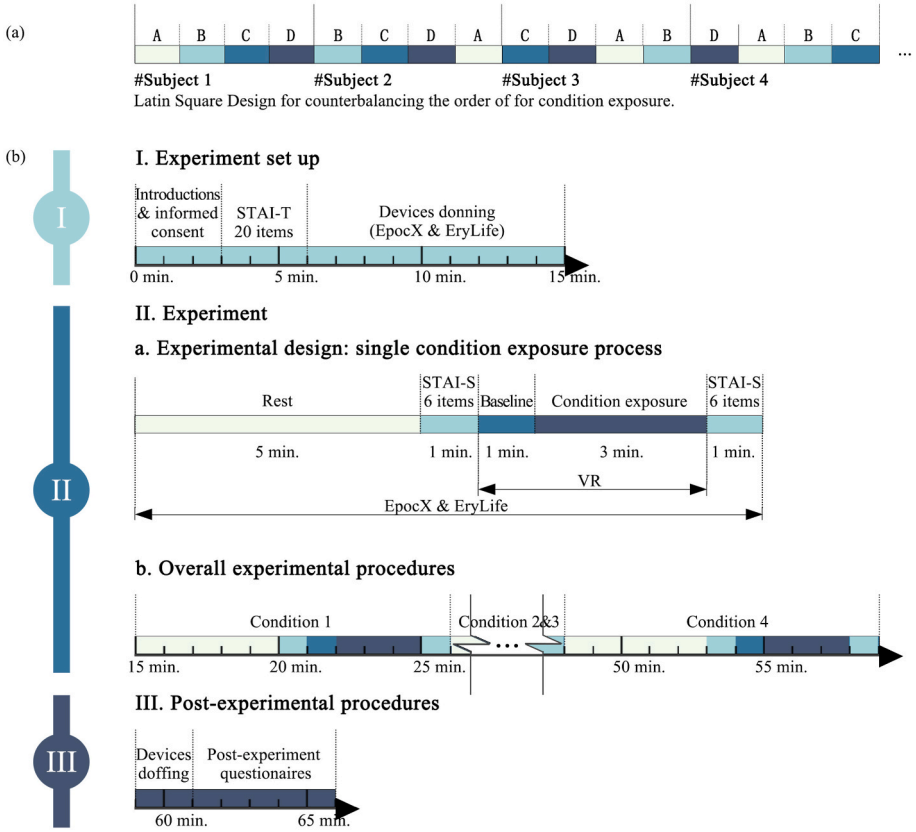


Fig. 3. (a) Experimental condition order counterbalanced with Latin Square Design. (b) Overview of the experimental procedure.

more than 20% of epochs were rejected. Finally, the EEG data were re-referenced to the average of all electrodes.

After preprocessing, the EEG data were transformed into the frequency domain. Power Spectral Density (PSD) of all the EEG data was calculated using the Multi-taper method, which reduces variance and spectral leakage (Prerau et al., 2017). During the calculation, the window length (N) was set to 2 s, and the number of tapers (K) was set to 3. Power values were calculated across the 1–40 Hz frequency range. Alpha band data (8–13 Hz) from F3 (left frontal) and F4 (right frontal) were extracted to compute Frontal Alpha Asymmetry (FAA). Because frontal alpha power is generally interpreted as inversely related to cortical activation, higher FAA values, calculated as ln (F4 alpha power) – ln (F3 alpha power), indicate relatively greater left frontal activation. Such a pattern has commonly been associated with approach-related affect, more positive emotional tendency, and adaptive emotional regulation. In contrast, lower or more negative FAA values indicate relatively greater right frontal activation, which has been linked to withdrawal-related affect, negative emotional tendency, and stress-related emotional states. In this study, FAA was used to reflect participants' frontal cortical asymmetry associated with emotional and stress-related responses to the VR environments (Ocklenburg et al., 2016; Giannakakis et al., 2022).

PPG signals were collected using EryLife S2, a wrist-worn multimodal signal acquisition device. This device recorded Blood Volume Pulse (BVP) signals using a Photoplethysmography (PPG) sensor, from which Inter-Beat Interval (IBI) sequences were extracted for HRV analysis. Data preprocessing was conducted using MATLAB 2023B and the HRVAS toolbox to identify and correct artifacts (Ramshur, 2010). HRVAS automatically detected and corrected IBI artifacts (e.g., from motion, poor sensor contact, ectopic beats) using threshold-based algorithms and interpolation from adjacent valid IBIs. Condition-level PPG recordings were excluded from the HRV analysis if more than 10% of IBIs required correction or were unrecoverable. Corrected data were used to derive Normal-to-Normal (NN) intervals to calculate the Root Mean Square of Successive Differences (RMSSD), an established indicator of parasympathetic nervous activity. Higher RMSSD values are associated with relaxation and lower stress (Shaffer and Ginsberg, 2017).

2.5. Amplitude spectrum slope ($-\alpha$) calculation

2.5.1. Image acquisition

To calculate the amplitude spectrum slope for each VR condition, images were rendered using Blender. In accordance with the ISO 7250-2 anthropometric database (ISO, 2024), the perceived eye height in a seated position was set at 770 mm (measured from the seat surface). The virtual camera was incrementally rotated by 5° along the horizontal axis, completing 72 steps to achieve full 360° horizontal scene coverage. Subsequently, a 5° vertical rotation was applied, and the horizontal rotation sequence was repeated. This process continued until the entire model was uniformly captured, resulting in 2592 rendered images per condition. These rendered images were used to characterize the SF properties of each VR condition.

To calculate the amplitude spectrum slope representing participants' personal views of the conditions, images of their views were recorded in real time using Unity during the experimental sessions. Screenshots were captured at two frames per second throughout each condition period. Each condition period yielded 360 images, resulting in a total of 1440 images per participant across the four condition periods. Personal α was calculated from these screenshots to summarize the SF structure of the scene content appearing in each participant's recorded views within each condition. The content of these views depends on both scene configuration and viewing direction during exposure. This approach allowed the spectral characteristics of each participant's recorded views to be examined in relation to physiological responses measured during the same exposure period. The methods of image acquisition for both the models and the participants' personal views are illustrated in Fig. 4.

2.5.2. Calculation of the amplitude spectrum slope

The process commenced with the input image being converted to grayscale by averaging its color channels. A two-dimensional Discrete Fourier Transform (DFT) was then applied to obtain the image's amplitude spectrum.

$$A(u,v) = \left|F_{\text{shift}}(u,v)\right|, F = \text{DFT}\{I\}. \tag{2}$$

Radial frequencies r (computed from the centered frequency coordinates after shifting the zero-frequency component to the spectrum center, with appropriate normalization) and their corresponding amplitudes A were extracted to form frequency–amplitude pairs. These pairs were binned by radial frequency, and the mean amplitude within each bin (A_k) was calculated to reduce noise and emphasize prevailing trends. Finally, the amplitude spectrum slope was estimated via linear regression in log–log space:

$$\log A_k = -\alpha \log r_k + c, \tag{3}$$

where A_k denotes the mean amplitude of bin k, r_k is the representative radial frequency of that bin, and α is the amplitude-spectrum decay exponent (i.e., the regression slope equals $-\alpha$). A larger α indicates a steeper decay of the amplitude spectrum.

2.6. Statistical analyses

To assess the effects of window shading and materiality on individual stress-related responses from an SF perspective, psychological and physiological measurements for each condition were first baseline-corrected. Linear Mixed Models (LMMs) were then fitted using the lme4 package for R. Age, gender, and STAI-T scores were included as covariates. Separate LMMs were specified using STAI-S, FAA, RMSSD, and preference rating as response variables. Window shading and materiality were dummy-coded, with closed blinds and artificial materiality as the reference categories. Gender was also dummy-coded, with female as the reference category. To control for the False Discovery Rate (FDR), all p-values were adjusted using the Benjamini-Hochberg method. The interaction between window shading and materiality was initially tested; because it was not statistically significant, the final models reported below included only the main effects. The model was formulated as follows:

$$Y_{ij} = \beta_0 + \beta_1 Win_{ij} + \beta_2 Mat_{ij} + \beta_3 Age_j + \beta_4 Gender_j + \beta_5 STAI - T_j + u_j + \epsilon_{ij} \tag{4}$$

Where Y_{ij} represents the outcome measure (STAI-S, FAA, RMSSD, or preference) for participant j under condition i; β_0 is the fixed intercept, representing the estimated mean of Y when materiality is "artificial", window shading is "closed", age is at its mean value after mean-centering, STAI-T is at zero on its original scale, and gender is at its reference category (female). $\beta_1 Win_{ij}$, $\beta_2 Mat_{ij}$, $\beta_3 Age_j$, $\beta_4 Gender_j$, and $\beta_5 STAI\text{-}T_j$ are included as fixed effects to capture the influence of window condition, materiality, age, gender, and STAI-T on the outcome. u_j is the random intercept for participant j, accounting for subject-specific deviations from the overall intercept, and ϵ_{ij} is the residual error for the i-th observation of participant j. Both u_j and ϵ_{ij} are assumed to be independently normally distributed with a mean of zero and variances σ_u^2 and σ_ϵ^2, respectively.

To investigate how window shading and materiality influenced the SF characteristics of participants' visual exposure, the personal α value for each participant under each condition was first summarized from the real-time screenshots captured during the corresponding VR exposure. These participant-by-condition α values were then mean-centered to obtain α_c. The centered α values were used as the response variable in an LMM with the same fixed-effect structure as Equation (4). In this case,

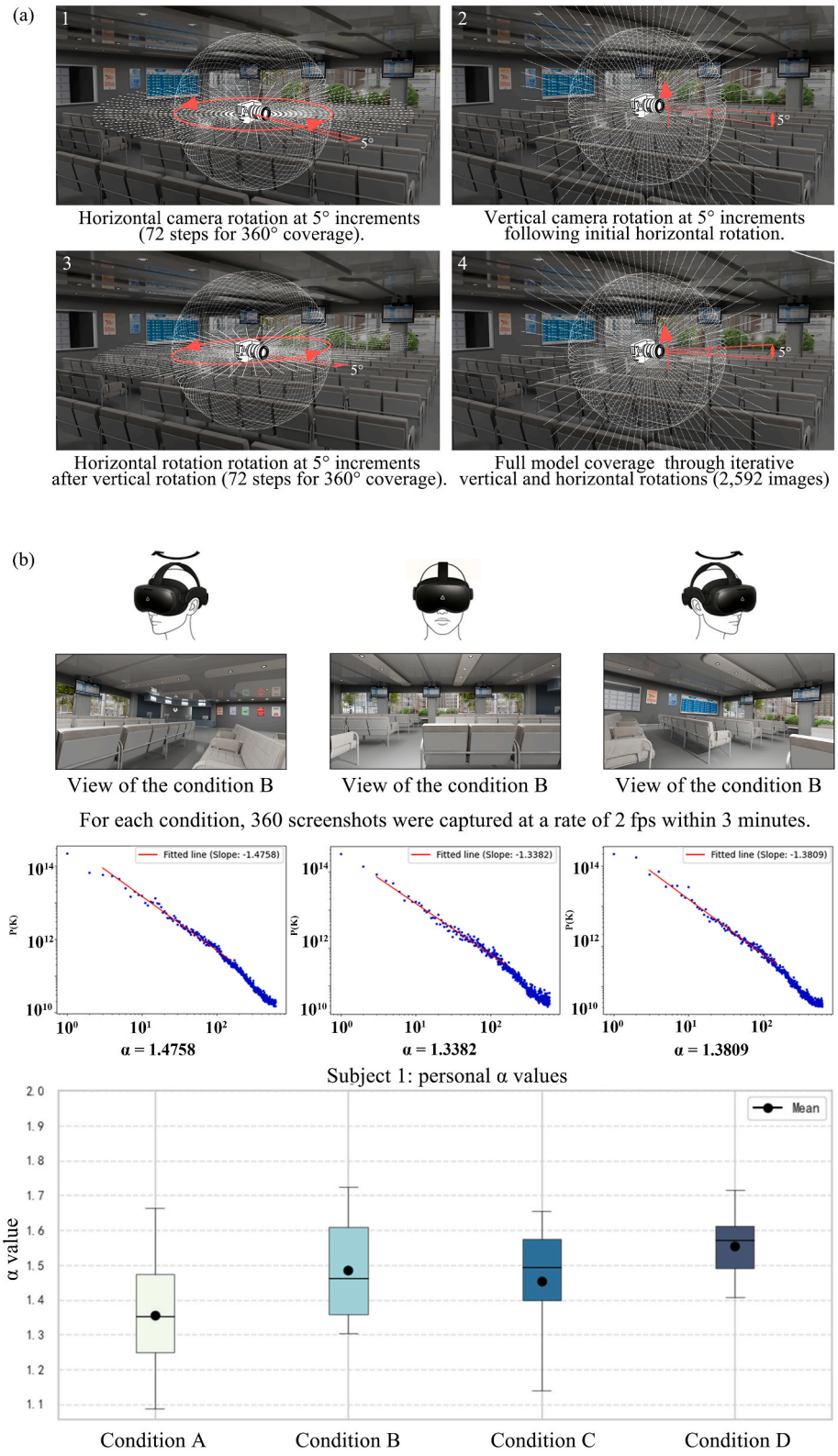


Fig. 4. (a) Rendered panoramas of each model used to compute amplitude spectrum slopes. (b) Real-time participant perspective screenshots of participants' views were captured during each condition for amplitude spectrum slope analysis.

the response variable Y_{ij} was defined as each participant's α_c values.

Next, to explore the within-subject correlation between α values and stress indicators, we used the repeated-measures correlation technique (rmcorr package in R) to account for the non-independence of observations.

Finally, to examine whether personal α_c values were associated with stress-related responses after controlling for covariates, we entered α_c as a fixed-effect predictor. Separate models were constructed using STAI-S, FAA, RMSSD, and preference as response variables. Age, gender, and STAI-T were included as covariates, with age mean-centered and gender

dummy-coded. The model was formulated as follows:

$$Y_{ij} = \beta_0 + \beta_1\alpha_{ij} + \beta_2 Age_j + \beta_3 Gender_j + \beta_4 STAI - T_j + u_j + \epsilon_{ij} \quad (5)$$

Where β_1 is the fixed-effect coefficient associated with α_{ij}, where α_{ij} denotes the personal α_c value for the i-th observation of participant j. Other parameters in this specification mirror those defined in Equation (4).

Model-derived α values were used to characterize the stimulus-level SF properties of the four VR conditions. This analysis was intended to document the spectral profiles of the standardized visual environments rather than to test participant-level hypotheses. Therefore, α values calculated from the 2592 rendered images per condition were summarized descriptively using the mean, standard deviation, and median, and reported in Table 2. These descriptive summaries provided a stimulus-level reference for interpreting the participant-view α values captured during the VR exposure. Inferential analyses involving α were based on participant-view α values, where each observation corresponded to one participant under one experimental condition.

3. Results

Baseline-corrected means and Standard Deviations (SD) for all psychological and physiological measures are presented in Table 2, and their distributions are depicted via boxplots in Fig. 5. Separate LMMs were fitted for each stress metric and preference rating to examine the effects of window shading and materiality; the fixed-effect estimates are reported in Table 3. In a subsequent series of LMMs, each participant's α_c values were included as a fixed predictor to explore their association with stress metrics and preference scores; these results are presented in Table 4.

3.1. The impact of window shading and materiality on stress-related responses

3.1.1. Psychological data

Baseline-corrected STAI-S scores, calculated as post-exposure minus pre-exposure mean-item scores, were modeled to examine the effects of window shading and materiality on state anxiety. Descriptive statistics showed that the Open Blinds + Biophilic Materiality condition yielded the smallest mean increase in STAI-S scores (0.099 ± 0.561), whereas the Closed Blinds + Artificial Materiality condition yielded the largest mean increase (0.844 ± 0.766).

The LMM confirmed significant main effects of both factors. Compared with closed blinds, open blinds were associated with a 0.30-point smaller increase in mean STAI-S scores (b = −0.30, 95%CI: −0.48 to −0.12, p < 0.001, β = −0.41). Compared with artificial materiality, biophilic materiality was associated with a 0.44-point smaller increase (b = −0.44, 95%CI: −0.62 to −0.27, p < 0.001, β = −0.61).

Among covariates, age was negatively associated with baseline-corrected STAI-S scores, with older participants showing smaller increases (b = −0.06, 95%CI: −0.10 to −0.01, p < 0.05, β = −0.19). STAI-T was also negatively associated with baseline-corrected STAI-S scores (b = −0.48, 95%CI: −0.75 to −0.21, p < 0.001, β = −0.28), indicating smaller STAI-S increases among participants with higher trait anxiety.

Preference ratings followed a parallel pattern. Both visual factors significantly influenced preference ratings (both p < 0.001). Open blinds increased preference relative to closed blinds (b = 1.21, 95%CI: 0.95 to 1.47, p < 0.001, β = 0.87), and biophilic-materiality conditions were strongly preferred over artificial-materiality conditions (b = 1.72, 95%CI: 1.46 to 1.98, p < 0.001, β = 1.23).

3.1.2. Physiological data

EEG data were band-pass filtered in the alpha range (8-13 Hz) to compute the FAA. Electrode sites and topographical distributions of alpha power across the four conditions are shown in Fig. 6. Results from the LMM indicated a significant effect of window shading on FAA: compared to the closed-blind condition, the open-blind condition significantly increased FAA (b = 0.10, 95%CI: 0.01 to 0.18, p < 0.05, β = 0.26). This pattern indicates relatively greater left frontal activation under the open-blind condition, which is commonly associated with approach-related affect, more positive emotional tendency, and adaptive emotional regulation. The effect of materiality trended in the expected direction, biophilic over artificial, but was not significant (b = 0.08, 95%CI: −0.01 to 0.16, p = 0.09, β = 0.21).

HRV was indexed by the RMSSD values. Higher RMSSD generally reflects greater parasympathetic activity and lower physiological arousal. The LMM results showed significant main effects of both factors: open blinds elevated RMSSD compared to closed blinds (b = 2.88 ms, 95%CI: 0.47 to 5.28, p < 0.05, β = 0.35) and biophilic materiality increased RMSSD relative to artificial materiality (b = 2.67ms, 95%CI: 0.26 to 5.07, p < 0.05, β = 0.33). These findings suggest that the open-blind and biophilic-materiality conditions were associated with stronger parasympathetic-related physiological responses.

3.2. The impact of window shading and materiality on personal α values

The personal amplitude spectrum slope was computed for each participant under each condition, and α_c values were used as the response variable in an LMM to examine how window shading and materiality influenced the SF characteristics of participants' visual exposure. The personal α values ranged from 1 to 2; after centering, the overall mean was 0. Smaller α_c values indicated that the original personal α values were closer to 1. The means and SDs of the personal α values for each condition are presented in Table 2. LMM results indicated significant effects of window shading (b = −0.10, 95%CI: −0.11 to −0.09, p < 0.001, β = −1.33) and materiality (b = −0.09, 95%CI: −0.10 to −0.08, p < 0.001, β = −1.15) on personal α values. These findings suggest that participants' visual exposure had lower α values under the open-blind and biophilic-materiality conditions, with Condition A yielding α values closest to 1.

Table 2
Descriptive statistics in psychological and physiological measurements.

Psychological indicators	Condition A Open blinds Biophilic materiality		Condition B Open blinds Artificial materiality		Condition C Closed blinds Biophilic materiality		Condition D Closed blinds Artificial materiality	
	Mean ± SD	Median	Mean ± SD	Median	Mean ± SD	Median	Mean ± SD	Median
STAI-S	0.099 ± 0.561	0	0.668 ± 0.747	0.666	0.525 ± 0.616	0.5	0.844 ± 0.766	0.833
Raw α data	1.36 ± 0.030	1.37	1.44 ± 0.048	1.44	1.46 ± 0.039	1.47	1.55 ± 0.020	1.55
Centered α data	−0.089 ± 0.030	−0.087	−0.011 ± 0.048	−0.013	0.002 ± 0.039	0.013	0.098 ± 0.020	0.097
α data of models	1.543 ± 0.132	1.542	1.613 ± 0.106	1.626	1.561 ± 0.134	1.560	1.633 ± 0.090	1.641
FAA	0.203 ± 0.419	0.098	0.069 ± 0.337	0.108	0.068 ± 0.379	0.0568	−0.026 ± 0.342	−0.024
RMSSD	7.02 ± 8.78	6.2	3.36 ± 7.85	1.85	3.16 ± 7.95	3.3	1.61 ± 7.42	2.4
Preferences	4.38 ± 0.848	5	2.64 ± 1.05	2	3.15 ± 1.04	3	1.45 ± 0.717	1

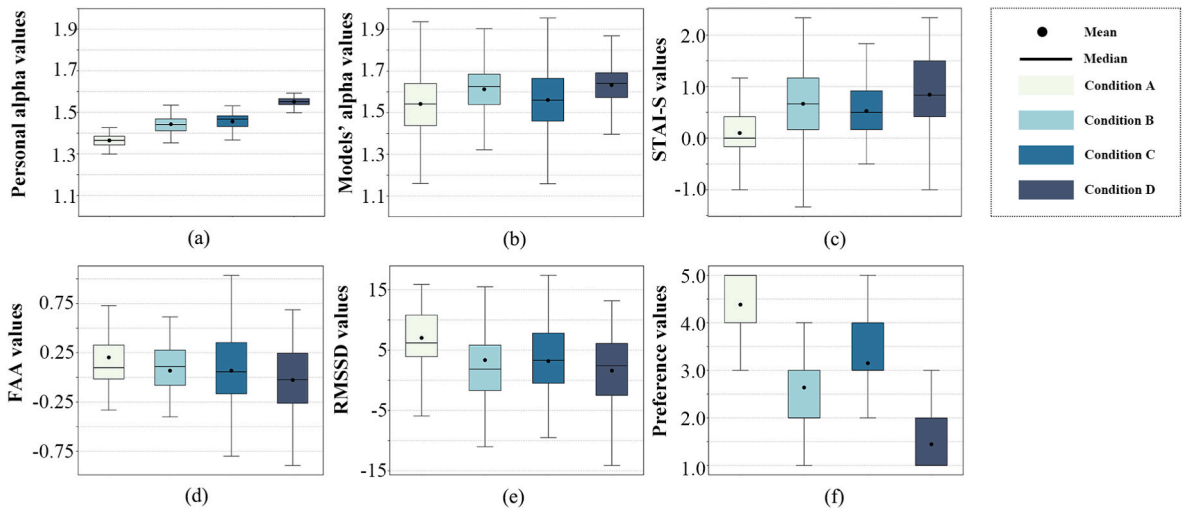


Fig. 5. Boxplot distributions of outcome measures across conditions: (a) Personal α values and (b) model-derived α values (both on the same scale); (c) STAI-S scores; (d) FAA; (e) RMSSD, and (f) condition preference ratings.

Table 3
Summary of LMM outcomes with window shading and materiality specified as fixed effects.

Measurement	n, Miss	Fixed effects (Coef. ± Std. Err., P-value)					
		Intercept	Open blinds	Biophilic materiality	STAI-T	Age	Gender
STAI-S	47, 0	1.870 ± 0.309***	−0.301 ± 0.089***	−0.444 ± 0.089***	−0.479 ± 0.136***	−0.057 ± 0.024*	0.188 ± 0.110
Preferences	47, 0	0.741 ± 0.394	1.212 ± 0.133***	1.723 ± 0.133***	0.332 ± 0.171	0.046 ± 0.030	−0.071 ± 0.139
RMSSD	47, 9%	7.960 ± 3.458*	2.877 ± 1.217*	2.665 ± 1.216*	−2.935 ± 1.505	−0.425 ± 1.505	−1.089 ± 1.221
FAA	47, 12%	0.197 ± 0.234	0.097 ± 0.043*	0.078 ± 0.043	−0.097 ± 0.103	−0.046 ± 0.018*	0.036 ± 0.084
α_c	47, 0	0.070 ± 0.018***	−0.100 ± 0.005***	−0.087 ± 0.005***	0.010 ± 0.008	0.002 ± 0.001	0.004 ± 0.007

*p < 0.05; **p < 0.01; ***p < 0.001. False Discovery Rate (FDR) adjusted. “n" indicates the sample size, and “Miss” refers to the ratio of missing observations.

Table 4
Summary of LMM outcomes when α_c is included as a fixed effect.

Measurement	n, Miss	Fixed effects (Coef. ± Std. Err., P-value)				
		Intercept	Personal-centered alpha	STAI-T	Age	Gender
STAI-S	47, 0	1.582 ± 0.310***	3.607 ± 0.598***	−0.514 ± 0.139***	−0.061 ± 0.025*	0.172 ± 0.113
Preferences	47, 0	1.935 ± 0.462***	−11.586 ± 1.060***	0.445 ± 0.171	0.066 ± 0.037	−0.021 ± 0.168
RMSSD	47, 9%	10.214 ± 3.378**	−22.957 ± 8.238**	−2.723 ± 1.510	−0.383 ± 0.268	−0.988 ± 1.226
FAA	47, 12%	0.264 ± 0.227	−0.916 ± 0.299**	−0.089 ± 0.102	−0.045 ± 0.018*	0.039 ± 0.083

*p < 0.05; **p < 0.01; ***p < 0.001. False Discovery Rate (FDR) adjusted. “n" indicates the sample size, and “Miss” refers to the ratio of missing observations.

3.3. Relationship between personal α values and stress metrics

Repeated-measures correlation analyses revealed significant associations between personal α values and both stress and preference outcomes. Specifically, higher α values correlated positively with STAI-S ($r = 0.46$, 95%CI: 0.32 to 0.58, $p < 0.001$) and negatively with FAA ($r = -0.23$, 95%CI: −0.39 to −0.05, $p < 0.05$), RMSSD ($r = -0.20$, 95% CI: −0.36 to −0.02, $p < 0.05$), and preference scores ($r = -0.70$, 95%CI: −0.76 to −0.61, $p < 0.001$). Trend plots are shown in Fig. 7. These findings suggest that, without controlling for covariates, original α values are significantly associated with stress measures and preference scores, though the associations with FAA and RMSSD were relatively modest.

Subsequently, α_c values were entered as fixed effects in separate LMMs, controlling for age, gender, and STAI-T, to examine associations with STAI-S, preference, FAA, and RMSSD. Personal α_c was significantly associated with each outcome in these models: a one-unit increase in α_c was associated with an increase in STAI-S of 3.61 (95%CI: 2.43 to 4.79, $p < 0.001$, $\beta = 0.38$), a decrease in preference scores of 11.59 (95%CI: −13.68 to −9.49, $p < 0.001$, $\beta = -0.63$), a decrease in FAA by 0.92 (95% CI: −1.51 to - 0.33, $p < 0.01$, $\beta = -0.18$), and a decrease in RMSSD by 22.96 (95%CI: −39.22 to −6.69, $p < 0.01$, $\beta = -0.21$). These findings demonstrate that increases in α_c are associated with significant elevations in STAI-S scores and significant reductions in FAA and RMSSD values, suggesting less favorable stress-related responses within the tested VR conditions.

LMM results are shown in Table 4. In summary, we first explored repeated correlation to assess the raw relationship between personal α values and stress-related metrics and then used α_c in LMMs to evaluate their associations. These results indicate that, within the tested VR conditions, personal α values closer to 1 were associated with lower STAI-S scores, higher FAA, higher RMSSD, and higher preference ratings. This suggests that the spectral characteristics of participants' recorded views, summarized by personal α, covaried with their stress-related and preference responses.

4. Discussion

This study investigated the impact of window shading and materiality on participants' stress-related psychological and physiological

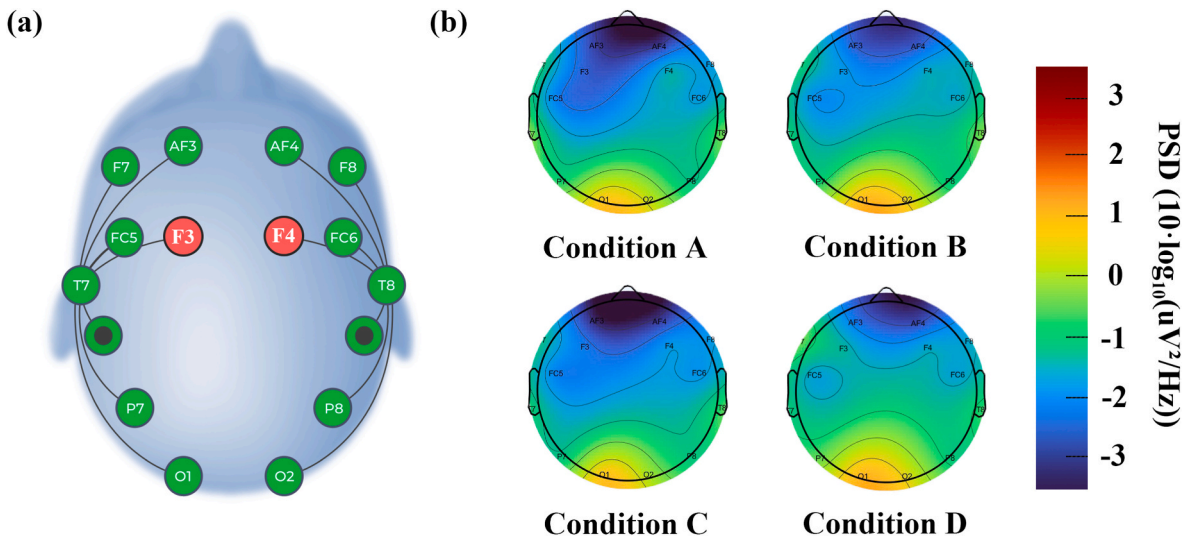


Fig. 6. (a) Emotiv Epoc X electrode montage with F3 and F4 (red) highlighted for FAA calculation. (b) Topographic maps of alpha-band PSD for the four conditions: A (Open Blinds + Biophilic Materiality), B (Open Blinds + Artificial Materiality), C (Closed Blinds + Biophilic Materiality), and D (Closed Blinds + Artificial Materiality). The color bar indicates PSD in 10·log10 (μV2/Hz), where warm colors (e.g., red) represent higher PSD values and cooler colors (e.g., blue) represent lower PSD values.

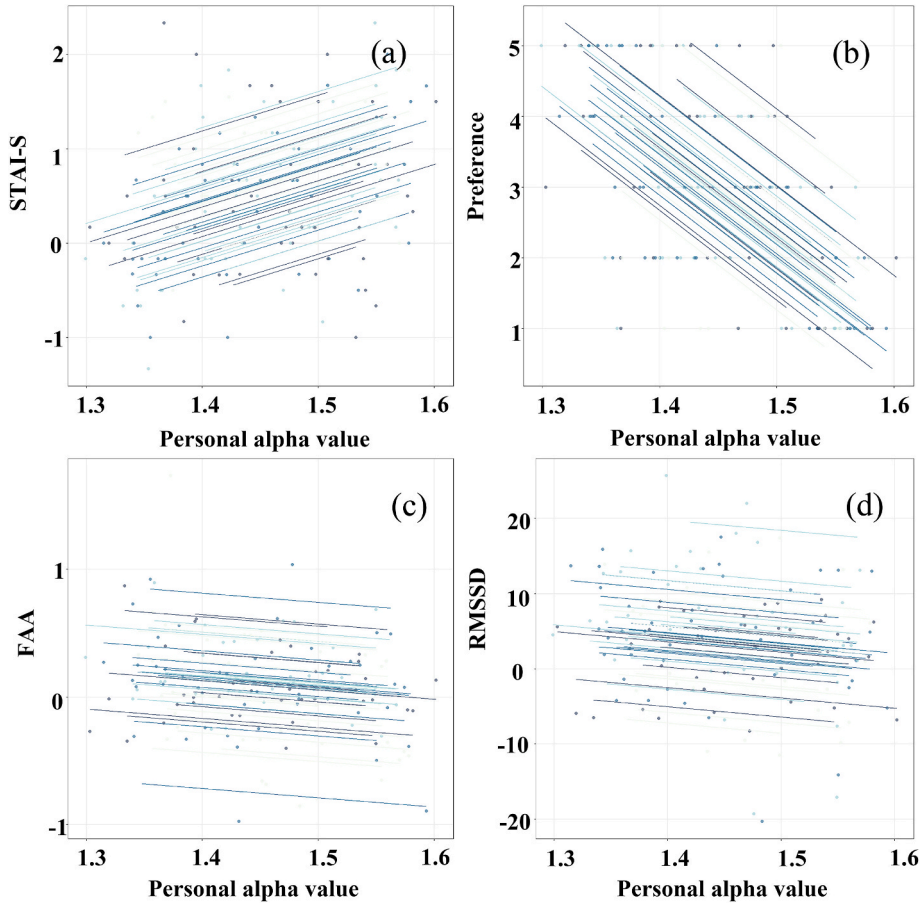


Fig. 7. Repeated measures correlations between personal α values and various measurement indices: (a) STAI-S, (b) preference ratings, (c) FAA, and (d) RMSSD (y-axis). Each point represents an observation for a single participant, and lines show the within-subject fitted relationship using a common group-level slope.

responses in VR-simulated hospital waiting areas from an SF perspective. The results showed that window shading and materiality significantly influenced STAI-S, RMSSD, preference ratings, and, in the case of window shading, FAA. In addition, personal α values were significantly associated with stress-related and preference responses. Specifically, personal α values closer to 1 were associated with lower STAI-S scores, higher FAA, higher RMSSD, and higher preference ratings within the tested VR conditions. These findings suggest that the spectral

characteristics of participants' recorded views, summarized by personal α, covaried with their psychological, physiological, and preference responses.

4.1. Influence of window shading and materiality on stress-related responses

Psychological stress was quantified using baseline-corrected STAI-S scores, calculated as post-exposure minus pre-exposure scores for each condition. After adjustment for age, gender, and STAI-T, open blinds and biophilic materiality were associated with smaller increases in mean STAI-S scores by 0.30 and 0.44 points, respectively, compared with closed blinds and artificial materiality. Preference scores mirrored these findings, with participants favoring the Open Blinds + Biophilic Materiality condition. Covariate effects showed that higher STAI-T and older age were associated with smaller pre-to-post increases in STAI-S scores, consistent with prior reports that chronic stress and aging attenuate sensitivity to acute stressors (Frankenhaeuser, 1986; Lupien et al., 2009).

Physiological measures corroborated the psychological results. FAA increased significantly under open-blind conditions, reflecting greater left-hemisphere activation, which is commonly associated with approach-related affect, more positive emotional tendency, and adaptive emotional regulation (Ocklenburg et al., 2016; Giannakakis et al., 2022). A similar trend was observed for biophilic materiality, though the effect was not significant. Open blinds and biophilic materiality were also associated with significantly larger baseline-corrected RMSSD changes by 2.88 and 2.67 ms, respectively, compared with closed blinds and artificial materiality. This pattern is consistent with more favorable parasympathetic-related responses (Shaffer and Ginsberg, 2017).

The larger RMSSD changes associated with open blinds are consistent in direction with Mihara et al. (2022), who reported higher RMSSD under window-view conditions than under closed-blind conditions in real and virtual office environments. The present findings show a similar response pattern in VR-simulated hospital waiting areas. For materiality, Kumpulainen et al. (2024) reported higher positive affect and lower negative affect in a wooden room than in a resin plaster room, broadly aligning with the more favorable subjective responses to biophilic materiality observed here. However, their study found no significant difference in RMSSD between material conditions, whereas a significant difference was observed in the present study.

Taken together, these findings suggest that open blinds and biophilic materiality supported more favorable psychological, physiological, and preference responses in the tested VR hospital waiting area environments. Open blinds may have contributed to these responses by increasing daylight availability, outdoor visibility, and perceived openness, which have been linked to positive emotions, reduced anxiety, and improved environmental satisfaction (Chang and Chen, 2005; Emami et al., 2024; Jiang et al., 2017). As for materiality, the responses observed under the wood-and-stone condition may be interpreted in relation to perceived warmth and restorative qualities (McGee et al., 2019), as well as the biophilia hypothesis (Kellert and Wilson, 1995). These perspectives offer possible explanations for the lower STAI-S scores, higher RMSSD, and higher preference ratings associated with the tested material palette as a whole. These interpretations should be understood at the level of integrated design conditions rather than as evidence for the independent contribution of any single perceptual attribute.

In summary, both psychological and physiological data consistently indicate that open blinds and biophilic materiality were associated with lower stress-related responses and higher user preference in VR-simulated hospital waiting areas. The physiological data, from the perspectives of frontal cortical asymmetry and parasympathetic-related activity, provided complementary evidence for understanding how visual environmental factors may influence participants' responses to healthcare waiting environments.

4.2. Associations of personal α with visual factors and stress-related responses

We used repeated correlations and LMMs to explore how α values were related to visual design factors, stress-related responses, and preference ratings. First, we modeled personal α_c values in an LMM, controlling for age, gender, and STAI-T. Both window shading (open vs. closed) and materiality (biophilic vs. artificial) significantly influenced the level of α_c: open blinds and biophilic materiality were associated with lower personal α_c values, indicating that these conditions altered the SF characteristics of the participants' visual exposure.

Next, repeated-measures correlations between the raw α data and both stress-related metrics and preference ratings confirmed significant associations: α correlated positively with STAI-S and negatively with FAA, RMSSD, and preference (though correlations with FAA and RMSSD were modest). Finally, separate LMMs examined the associations between personal α_c and the response variables, adjusting for age, gender, and STAI-T. These associations were statistically significant.

These findings suggest that, within the tested VR conditions, the spectral characteristics of participants' recorded views, summarized by personal α, were associated with their psychological, physiological, and preference responses. In this study, α was treated as an image-based descriptor rather than as a separate design variable, helping to characterize the SF structure of the recorded scene content under the different window-shading and materiality conditions.

In summary, window shading and materiality influenced SF characteristics of participants' visual exposure, as reflected by personal α values. Personal α values closer to 1 were associated with more favorable responses, including lower STAI-S scores, higher FAA, higher RMSSD, and higher preference ratings. These results support the use of α as an image-based spectral descriptor for characterizing visual scene structure in relation to stress-related responses in VR-simulated healthcare waiting environments.

4.3. Personal α values closer to 1 and more favorable stress-related responses

By relating personal α values to stress-related measures and preference ratings, this study found that, within the tested VR conditions, personal α values closer to 1 were associated with lower STAI-S scores, higher FAA, higher RMSSD, and higher preference ratings. Because the original personal α values in this study ranged from 1 to 2, lower α_c values indicated that the corresponding original α values were closer to 1. Thus, lower α_c values were associated with more favorable psychological, physiological, and preference responses.

The parameter α describes the decay of SF amplitude in environmental images, reflecting the distribution between LSF, such as global layout and large-scale structures, and HSF, like edges and textures. Both LSF and HSF are crucial for scene recognition (Loftus and Harley, 2004). An optimal balance supports effective perception; if α is excessively high (e.g., around 2), HSF decays rapidly, leading to a loss of image detail. Therefore, α provides a compact descriptor of how visual information is distributed across spatial scales.

Natural images typically exhibit α values around 1 (Field, 1987). This indicates a balanced SF distribution with strong low-frequency energy and a gradual decline in high-frequency content, providing scale-invariant perceptual information associated with visual comfort (Field, 1987; Stephens et al., 2013). This distribution aligns well with the human visual system. According to the Efficient Coding Hypothesis, such 1/f patterns support efficient, low-redundancy processing in the human visual system and are often perceived as more comfortable and aesthetically pleasing (Barlow, 1961; Simoncelli and Olshausen, 2001; Fernandez and Wilkins, 2008). From this perspective, visual environments with α values closer to 1 may be easier to process and may be experienced as more visually comfortable.

The personal α findings are broadly consistent with Juricevic et al.

(2010b), who reported lower visual discomfort for synthetic images with approximately 1/f luminance amplitude spectra. Similarly, within the observed range of 1–2, personal α values closer to 1 were associated with more favorable stress-related responses in the present study. Whereas their study manipulated the spectra of synthetic images and assessed visual discomfort, our study examined associations between spectral characteristics calculated from participants' recorded VR views and psychological and physiological responses in hospital waiting areas.

In the present study, Condition A (Open Blinds + Biophilic Materiality) produced personal α values closest to 1 and was associated with the most favorable overall response pattern. These findings suggest that the SF characteristics captured by α provide a useful way to describe SF differences among visual design conditions that were experienced more favorably.

In conclusion, personal α values closer to 1 were associated with more favorable stress-related and preference responses within the tested VR-simulated hospital waiting areas. These findings suggest that the amplitude spectrum slope can serve as an image-based spectral descriptor for characterizing visual scene structure in relation to visual IEQ and user responses.

4.4. The implications for research and design

This study provides a quantitative spectral perspective on hospital waiting-area design by relating personal α, calculated from participants' recorded views, to psychological, physiological, and preference responses under different window-shading and materiality conditions. By calculating the amplitude spectrum slope of the perceived scenes, we quantified the SF characteristics of the scenes viewed by participants and examined their associations with psychological and physiological stress-related responses. In addition, model-derived α values provided a stimulus-level description of the standardized VR conditions. Together, these two types of α measurements helped characterize how window shading and materiality shaped the visual structure of the simulated waiting areas.

These findings offer practical implications for interior design, particularly in high-stress settings such as hospital waiting areas. The Open Blinds + Biophilic Materiality condition produced α values closest to 1 and was associated with the most favorable overall response pattern. This suggests that integrated visual strategies involving window openness, daylight access, outdoor views, and natural materiality may create visual environments whose SF characteristics are more similar to those commonly observed in natural scenes (Simoncelli and Olshausen, 2001). These strategies have been widely discussed in healthcare and biophilic design research (Wilkins, 2016; Jimenez et al., 2021). The present findings further suggest that SF analysis can provide a quantitative, image-based descriptor of their visual scene structure. In this sense, α may complement existing visual IEQ assessments and help researchers and designers interpret how window shading and materiality relate to users' psychological, physiological, and preference responses. More broadly, such quantitative descriptors could be integrated into hospital design support system architectures to provide measurable visual-environment inputs for evidence-based healthcare design decision-making (Jia et al., 2026).

5. Limitations

This study investigated the effects of window shading and materiality on individuals' stress-related responses in a VR-simulated hospital waiting area and examined these responses in relation to the SF characteristics of the visual scenes. However, several limitations warrant consideration.

First, the technical limitations of VR simulation may have affected the experimental results. This study used VR to simulate real-world environments. Although prior research supports the validity of VR simulations for eliciting comparable psychological and physiological outcomes to those in physical environments (Higuera-Trujillo et al., 2017), VR cannot fully replicate real-world environments, particularly with respect to model texture fidelity and the ambient lighting complexity. Additionally, the display resolution of the HTC Vive Focus 3 used in this study may not perfectly reproduce the visual contrast and clarity of natural scenes. Consequently, participants' perceptions of visual stimuli may differ from those in real-world waiting areas, potentially limiting the generalizability and ecological validity of findings. Moreover, prolonged VR immersion may lead to physical discomfort, including nausea and headaches, which are rare in real-world environments.

Secondly, our participant cohort consisted mainly of healthy young adults, restricting the applicability of the findings to clinical populations. Although participants were instructed to imagine themselves waiting in a hospital waiting area for a routine consultation, their psychological state likely differs from the complex emotional experiences encountered by actual patients or visitors experiencing uncertainty, illness-related concerns, or medical decision-making. Future research should validate these findings in real clinical environments with diverse samples.

Finally, the α–response associations were examined within a limited set of VR waiting-area environments. Although the present findings support α as an image-based spectral descriptor and quantitative reference for visual IEQ assessment, its generalizability across broader and independent visual environments requires further validation.

6. Conclusions

This study employed VR to simulate a hospital waiting area while recording participants' psychophysiological data to investigate how window shading and materiality were associated with stress-related responses and SF characteristics, as quantified by the amplitude spectrum slope (-α).

In the tested sample of 47 healthy young adults, open blinds and biophilic materiality were associated with lower baseline-corrected STAI-S scores than closed blinds and artificial materiality, respectively ($b = -0.301$, 95% CI: -0.48 to -0.12; $b = -0.444$, 95% CI: -0.62 to -0.27). Corresponding differences in baseline-corrected RMSSD were +2.877 ms (95%CI: 0.47 to 5.28) and +2.665 ms (95%CI: 0.26 to 5.07). Preference ratings were higher by 1.212 and 1.723 points, respectively. Open blinds were also associated with higher baseline-corrected FAA ($b = 0.097$), whereas the materiality effect was not statistically significant ($b = 0.078$, $p = 0.09$).

Open blinds and biophilic materiality were also associated with lower personal α ($b = -0.100$ and -0.087, respectively). In separate mixed models adjusted for age, gender, and STAI-T, higher personal α was associated with higher baseline-corrected STAI-S ($b = 3.607$, 95% CI: 2.43 to 4.79) and lower baseline-corrected RMSSD ($b = -22.957$ ms, 95% CI: -39.22 to -6.69). Negative associations were also observed for FAA ($b = -0.916$) and preference ($b = -11.586$). Personal α summarized the spectral characteristics of participants' recorded views, while model-derived α provided descriptive profiles of the standardized VR scenes. These findings support α as an image-based spectral descriptor for relating visual scene structure to participant responses.

By integrating SF analysis with psychological and physiological measurements, this study provides a quantitative approach for evaluating visual IEQ in healthcare waiting environments. The amplitude spectrum slope may provide a quantitative reference for understanding how visual design factors such as window shading and materiality shape users' experiences. Future research may extend this approach to additional visual variables, more diverse participant groups, and real-world healthcare settings.

CRediT authorship contribution statement

Mirna Zordan: Writing – review & editing, Writing – original draft,

Supervision, Resources, Project administration, Methodology, Investigation, Funding acquisition, Conceptualization. **Zixian Lei:** Writing – review & editing, Writing – original draft, Visualization, Validation, Software, Methodology, Formal analysis, Data curation. **Jiakun Pei:** Writing – review & editing, Visualization, Validation, Investigation.

Declaration of generative AI and AI-assisted technologies in the writing process

During the preparation of this work, the authors used DeepSeek to improve the readability and language of the manuscript. After using this tool, the authors reviewed and edited the content as needed and take full responsibility for the content of the publication.

Funding

This work was supported by the National Natural Science Foundation of China (NSFC) under the Grant No. W2533138.

Declaration of competing interest

The authors declare that they have no known competing financial interests or personal relationships that could have appeared to influence the work reported in this paper.

Acknowledgements

The authors would like to express their sincere gratitude to the National Natural Science Foundation of China for the financial support to carry out the research work. The authors would also like to deeply thank Mr. Piet Maree for his continuous insights and inspiration, and to Ms. Lu Lin for her contribution as a research assistant during the development of this research.

Appendix A. Supplementary data

Supplementary data to this article can be found online at https://doi.org/10.1016/j.dibe.2026.101070.

Data availability

Data will be made available on request.

References

Barlow, H.B., 1961. Possible principles underlying the transformation of sensory messages. Sens. Commun. 1, 217–233.
Berlyne, D.E., 1960. Conflict, Arousal, and Curiosity.
Beukeboom, C.J., Langeveld, D., Tanja-Dijkstra, K., 2012. Stress-reducing effects of real and artificial nature in a hospital waiting room. J. Alternative Compl. Med. 18, 329–333. https://doi.org/10.1089/acm.2011.0488.
Bex, P.J., Makous, W., 2002. Spatial frequency, phase, and the contrast of natural images. J. Opt. Soc. Am. A 19, 1096. https://doi.org/10.1364/JOSAA.19.001096.
Bullier, J., 2001. Integrated model of visual processing. Brain Res. Rev. 36, 96–107. https://doi.org/10.1016/S0165-0173(01)00085-6.
Cardaci, M., Di Gesù, V., Petrou, M., Tabacchi, M.E., 2009. A fuzzy approach to the evaluation of image complexity. Fuzzy Set Syst. 160, 1474–1484. https://doi.org/10.1016/j.fss.2008.11.017.
Cavalcante, A., Mansouri, A., Kacha, L., Barros, A.K., Takeuchi, Y., Matsumoto, N., Ohnishi, N., 2014. Measuring streetscape complexity based on the statistics of local contrast and spatial frequency. PLoS One 9, e87097. https://doi.org/10.1371/journal.pone.0087097.
Chang, C.-Y., Chen, P.-K., 2005. Human response to window views and indoor plants in the workplace. HortSci 40, 1354–1359. https://doi.org/10.21273/HORTSCI.40.5.1354.
CIBSE, 2014. Lighting guide 10: daylighting—A guide for designers. In: Chartered Institution of Building Services Engineers.
Cohen, J., 2013. Statistical Power Analysis for the Behavioral Sciences, 0 ed. Routledge. https://doi.org/10.4324/9780203771587.
Dansky, K.H., Miles, J., 1997. Patient satisfaction with ambulatory healthcare services: waiting time and filling time. J. Healthc. Manag. 42, 165–177.
Delorme, A., Makeig, S., 2004. EEGLAB: an open source toolbox for analysis of single-trial EEG dynamics including independent component analysis. J. Neurosci. Methods 134, 9–21. https://doi.org/10.1016/j.jneumeth.2003.10.009.
Donderi, D.C., 2006. Visual complexity: a review. Psychol. Bull. 132, 73–97. https://doi.org/10.1037/0033-2909.132.1.73.
Du, M., Zhang, Y., Zhang, X., Tang, Z., Zhai, M., Hong, B., 2025. Floral walls versus green wall for stress recovery and cognitive restoration in underground environments: a VR-based experimental study. Dev. Built Environ. 24, 100819. https://doi.org/10.1016/j.dibe.2025.100819.
Durmus, D., 2020. Spatial frequency and the performance of image-based visual complexity metrics. IEEE Access 8, 100111–100119. https://doi.org/10.1109/ACCESS.2020.2998292.
Emami, M., Pazhouhanfar, M., Stoltz, J., 2024. Evaluating patients' preferences for dental clinic waiting area design and the impact on perceived stress. Buildings 14, 3160. https://doi.org/10.3390/buildings14103160.
EN 17037: Daylight in Buildings, 2018.
Esco, M.R., Flatt, A.A., 2014. Ultra-short-term heart rate variability indexes at rest and post-exercise in athletes: evaluating the agreement with accepted recommendations. J. Sports Sci. Med. 13, 535–541.
Evans, G.W., 1984. Environmental Stress. CUP Archive.
Evans, G.W., 2003. The built environment and mental health. J. Urban Health: Bull. N. Y. Acad. Med. 80, 536–555. https://doi.org/10.1093/jurban/jtg063.
Evans, G.W., McCoy, J.M., 1998. When buildings DON'T work: the role of architecture in human health. J. Environ. Psychol. 18, 85–94. https://doi.org/10.1006/jevp.1998.0089.
Faul, F., Erdfelder, E., Buchner, A., Lang, A.-G., 2009. Statistical power analyses using G*Power 3.1: tests for correlation and regression analyses. Behav. Res. Methods 41, 1149–1160. https://doi.org/10.3758/BRM.41.4.1149.
Fechner, G.T., 1948. Elements of Psychophysics.
Fernandez, D., Wilkins, A.J., 2008. Uncomfortable images in art and nature. Perception 37, 1098–1113. https://doi.org/10.1068/p5814.
Field, D.J., 1987. Relations between the statistics of natural images and the response properties of cortical cells. J. Opt. Soc. Am. A 4, 2379. https://doi.org/10.1364/JOSAA.4.002379.
Frankenhaeuser, M., 1986. A psychobiological framework for research on human stress and coping. In: Dynamics of Stress: Physiological, Psychological and Social Perspectives. Springer, pp. 101–116.
Garciai, K.D., Wierwille, W.W., 1985. Effect of glare on performance of a VDT reading-comprehension task. Hum. Factors 27, 163–173. https://doi.org/10.1177/001872088502700204.
Giannakakis, G., Grigoriadis, D., Giannakaki, K., Simantiraki, O., Roniotis, A., Tsiknakis, M., 2022. Review on psychological stress detection using biosignals. IEEE Trans. Affective Comput. 13, 440–460. https://doi.org/10.1109/TAFFC.2019.2927337.
Gibson, J.J., 2014. The Ecological Approach to Visual Perception, Classic. Psychology press.
Gong, Y., Qiu, M., Huo, F., 2023. Research on the efficiency of visual search for car interface icons based on visual complexity and spatial frequency. J. Computer-Aided Des. Comput. Graph. 35, 1612–1619. https://doi.org/10.3724/SP.J.1089.2023.19591.
Guo, F., Luo, M., Zhao, H., Du, Z., Zhang, Z., Zhang, H., Dong, J., Zhang, D., 2024. Qualitative mechanisms of perceived indoor environmental quality on anxiety symptoms in university. Buildings 14, 3530. https://doi.org/10.3390/buildings14113530.
Hall, C., Knuth, M., 2019. An update of the literature supporting the well-being benefits of plants: a review of the emotional and mental health benefits of plants. J. Environ. Hortic. 37, 30–38. https://doi.org/10.24266/0738-2898-37.1.30.
Higuera-Trujillo, J.L., López-Tarruella Maldonado, J., Llinares Millán, C., 2017. Psychological and physiological human responses to simulated and real environments: a comparison between photographs, 360° panoramas, and virtual reality. Appl. Ergon. 65, 398–409. https://doi.org/10.1016/j.apergo.2017.05.006.
Hochberg, J.E., 1957. Effects of the gestalt revolution: the cornell symposium on perception. Psychol. Rev. 64, 73–84. https://doi.org/10.1037/h0043738.
Isherwood, Z.J., Schira, M.M., Spehar, B., 2017. The tuning of human visual cortex to variations in the 1/fα amplitude spectra and fractal properties of synthetic noise images. Neuroimage 146, 642–657. https://doi.org/10.1016/j.neuroimage.2016.10.013.
ISO, I., 2024. 7250-2: Basic Human Body Measurements for Technological design-part 2: Body Measurement Definitions and Landmarks. International Organization for Standardization, Geneva, Switzerland.
Jacquin, A.E., 1992. Image coding based on a fractal theory of iterated contractive image transformations. IEEE Trans. Image Process. 1, 18–30. https://doi.org/10.1109/83.128028.
Jafarifiroozabadi, R., 2025. Investigating the impact of window features and room layout on anxiety, depression, and analgesic medication intake among patients: a pilot study in a cardiac intensive care unit. HERD 18, 14–30. https://doi.org/10.1177/19375867251314518.
Jafarifiroozabadi, R., Woo, M., Joseph, A., MacNaughton, P., Mihandoust, S., 2022. The effects of window blind positions and control on patients' hospital and care quality perception: a mediation and moderation analysis. Build. Environ. 226, 109672. https://doi.org/10.1016/j.buildenv.2022.109672.
Jia, Z., Nourian, P., Luscuere, P., Wagenaar, C., 2026. HDSS: a hospital design support system architecture. Dev. Built Environ. 26, 100916. https://doi.org/10.1016/j.dibe.2026.100916.

Jiang, S., Powers, M., Allison, D., Vincent, E., 2017. Informing healthcare waiting area design using transparency attributes: a comparative preference study. HERD 10, 49–63. https://doi.org/10.1177/1937586716675581.
Jimenez, M.P., DeVille, N.V., Elliott, E.G., Schiff, J.E., Wilt, G.E., Hart, J.E., James, P., 2021. Associations between nature exposure and health: a review of the evidence. IJERPH 18, 4790. https://doi.org/10.3390/ijerph18094790.
Juricevic, I., Land, L., Wilkins, A., Webster, M.A., 2010a. Visual discomfort and natural image statistics. Perception 39, 884–899. https://doi.org/10.1068/p6656.
Juricevic, I., Land, L., Wilkins, A., Webster, M.A., 2010b. Visual discomfort and natural image statistics. Perception 39, 884–899. https://doi.org/10.1068/p6656.
Kawamoto, N., 2002. Visual complexity and beauty of colored mosaic patterns on a CRT display. Sen-i Gakkaishi 58, 387–394. https://doi.org/10.2115/fiber.58.387.
Kellert, S.R., 2008. Dimensions, elements, and attributes of biophilic design. In: Kellert, S.R., Heerwagen, J.H., Mador, M.L. (Eds.), Biophilic Design: the Theory, Science and Practice of Bringing Buildings to Life. Wiley, Hoboken, N.J., pp. 3–19
Kellert, S.R., Calabrese, E.F., 2015. In: The Practice of Biophilic Design. https://www.biophilic-design.com/_files/ugd/21459d_81ccb84caf6d4bee8195f9b5af92d8f4.pdf.
Kellert, S.R., Wilson, E.O., 1995. The Biophilia Hypothesis.
Khodakarami, J., Nasrollahi, N., 2012. Thermal comfort in hospitals – a literature review. Renew. Sustain. Energy Rev. 16, 4071–4077. https://doi.org/10.1016/j.rser.2012.03.054.
Kim, S., 2025. Cognitive efficiency in VR simulated natural indoor environments examined through EEG and affective responses. Sci. Rep. 15, 33398. https://doi.org/10.1038/s41598-025-18629-z.
Kumpulainen, S., Kilpiäinen, M., Koski, J., Pesola, A.J., 2024. Wooden interiors improve heart rate variability-derived psychophysiological well-being: an acute cross-over study. Environ. Behav. 56, 155–178. https://doi.org/10.1177/00139165241270631.
Lee, J.H., Ostwald, M.J., 2023. The 'visual attractiveness' of architectural facades: measuring visual complexity and attractive strength in architecture. Archit. Sci. Rev. 66, 42–52. https://doi.org/10.1080/00038628.2022.2137458.
Li, J., Wu, J., Lam, F., Zhang, C., Kang, J., Xu, H., 2021. Effect of the degree of wood use on the visual psychological response of wooden indoor spaces. Wood Sci. Technol. 55, 1485–1508. https://doi.org/10.1007/s00226-021-01320-7.
Li, X., Zhang, C., Li, W., Ricard, R., Meng, Q., Zhang, W., 2015. Assessing street-level urban greenery using google street view and a modified green view index. Urban For. Urban Green. 14, 675–685. https://doi.org/10.1016/j.ufug.2015.06.006.
Lipovac, D., Burnard, M.D., 2021. Effects of visual exposure to wood on human affective states, physiological arousal and cognitive performance: a systematic review of randomized trials. Indoor Built Environ. 30, 1021–1041. https://doi.org/10.1177/1420326X20927437.
Loftus, G.R., Harley, E.M., 2004. How different spatial-frequency components contribute to visual information acquisition. J. Exp. Psychol. Hum. Percept. Perform. 30, 104–118. https://doi.org/10.1037/0096-1523.30.1.104.
Lundberg, A., Hillebrecht, A.-L., Srinivasan, M., 2024. Effect of waiting room ambience on the stress and anxiety of patients undergoing medical treatment: a systematic review and meta-analysis. Adv. Integrat. Med. 11, 47–68. https://doi.org/10.1016/j.aimed.2024.04.004.
Lupien, S.J., McEwen, B.S., Gunnar, M.R., Heim, C., 2009. Effects of stress throughout the lifespan on the brain, behaviour and cognition. Nat. Rev. Neurosci. 10, 434–445. https://doi.org/10.1038/nrn2639.
Ma, L., He, S., Lu, M., 2021. A measurement of visual complexity for heterogeneity in the built environment based on fractal dimension and its application in two gardens. Fractal Fract. 5, 278. https://doi.org/10.3390/fractalfract5040278.
Manu, S., Burgholz, T.M., Nabilou, F., Rewitz, K., El-Mokadem, M., Yadav, M., Chinazzo, G., Forgiarini Rupp, R., Azar, E., Syndicus, M., Sadick, A.-M., Schweiker, M., Crosby, S., Kong, M., Vakalis, D., Rysanek, A., Müller, D., Fels, J., Van Treeck, C., Frisch, J., Christoforou, R., 2024. A state-of-the-art, systematic review of indoor environmental quality studies in work-from-home settings. Build. Environ. 259, 111652. https://doi.org/10.1016/j.buildenv.2024.111652.
Marteau, T.M., Bekker, H., 1992. The development of a six-item short-form of the state scale of the spielberger state—trait anxiety inventory (STAI). Br. J. Clin. Psychol. 31, 301–306. https://doi.org/10.1111/j.2044-8260.1992.tb00997.x.
McGee, B., Park, N., Portillo, M., Bosch, S., Swisher, M., 2019. Diy biophilia: development of the biophilic interior design matrix as a design tool. J. Inter. Des. 44, 201–221. https://doi.org/10.1111/joid.12159.
Mihara, K., Hasama, T., Takasuna, H., 2022. Physiological and psychological responses and cognitive performance with a window view. Sci. Technol. Built Environ. 28, 547–556. https://doi.org/10.1080/23744731.2022.2049639.
Mott, M.S., Thomas, T.R., Burnette, J.L., 2013. Leveraging lighting color, temperature and luminosity for improving classroom learning. Networks: Online J. Teacher Res. 15. https://doi.org/10.4148/2470-6353.1059, 486–486.
Mourshed, M., Zhao, Y., 2012. Healthcare providers' perception of design factors related to physical environments in hospitals. J. Environ. Psychol. 32, 362–370. https://doi.org/10.1016/j.jenvp.2012.06.004.
Munoz, M.L., Van Roon, A., Riese, H., Thio, C., Oostenbroek, E., Westrik, I., De Geus, E.J. C., Gansevoort, R., Lefrandt, J., Nolte, I.M., Snieder, H., 2015. Validity of (Ultra-) Short recordings for heart rate variability measurements. PLoS One 10, e0138921. https://doi.org/10.1371/journal.pone.0138921.
Nimlyat, P.S., Kandar, M.Z., 2015. Appraisal of indoor environmental quality (IEQ) in healthcare facilities: a literature review. Sustain. Cities Soc. 17, 61–68. https://doi.org/10.1016/j.scs.2015.04.002.
Ochoa, C.E., Capeluto, I.G., 2006. Evaluating visual comfort and performance of three natural lighting systems for deep office buildings in highly luminous climates. Build. Environ. 41, 1128–1135. https://doi.org/10.1016/j.buildenv.2005.05.001.
Ocklenburg, S., Korte, S.M., Peterburs, J., Wolf, O.T., Güntürkün, O., 2016. Stress and laterality – the comparative perspective. Physiol. Behav. 164, 321–329. https://doi.org/10.1016/j.physbeh.2016.06.020.
Ohta, H., Maruyama, M., Tanabe, Y., Hara, T., Nishino, Y., Tsujino, Y., Morita, E., Kobayashi, S., Shido, O., 2008. Effects of redecoration of a hospital isolation room with natural materials on stress levels of denizens in cold season. Int. J. Biometeorol. 52, 331–340. https://doi.org/10.1007/s00484-007-0125-4.
Olivia, A., Mack, M.L., Shrestha, M., Peeper, A., 2004. Identifying the perceptual dimensions of visual complexity of scenes. Proc. Ann. Meet. Cognit. Sci. Soc. 26.
Posner, M.I., Nissen, M.J., Klein, R.M., 1976. Visual dominance: an information-processing account of its origins and significance. Psychol. Rev. 83, 157–171. https://doi.org/10.1037/0033-295X.83.2.157.
Prerau, M.J., Brown, R.E., Bianchi, M.T., Ellenbogen, J.M., Purdon, P.L., 2017. Sleep neurophysiological dynamics through the lens of multitaper spectral analysis. Physiology 32, 60–92. https://doi.org/10.1152/physiol.00062.2015.
Ramshur Jr., J.T., 2010. Design, Evaluation, and Application of Heart Rate Variability Analysis Software (Hrvas.
Rigau, J., Feixas, M., Sbert, M., 2005. An information-theoretic framework for image complexity. In: Proceedings of the First Eurographics Conference on Computational Aesthetics in Graphics, Visualization and Imaging, pp. 177–184.
Rus, T., Cruciat, G., Nemeti, G., Mare, R., Muresan, D., 2022. Thermal comfort in maternity wards: summer vs. winter conditions. J. Build. Eng. 51, 104356. https://doi.org/10.1016/j.jobe.2022.104356.
Seiferling, I., Naik, N., Ratti, C., Proulx, R., 2017. Green streets – quantifying and mapping urban trees with street-level imagery and computer vision. Landsc. Urban Plann. 165, 93–101. https://doi.org/10.1016/j.landurbplan.2017.05.010.
Shaffer, F., Ginsberg, J.P., 2017. An overview of heart rate variability metrics and norms. Front. Public Health 5, 258. https://doi.org/10.3389/fpubh.2017.00258.
Simoncelli, E.P., Olshausen, B.A., 2001. Natural image statistics and neural representation. Annu. Rev. Neurosci. 24, 1193–1216. https://doi.org/10.1146/annurev.neuro.24.1.1193.
Spielberger, C.D., Gonzalez-Reigosa, F., Martinez-Urrutia, A., Natalicio, L.F., Natalicio, D.S., 1971. The state-trait anxiety inventory. Revis. Interam. Psicol./Interam. J. Psychol. 5.
Stephens, G.J., Mora, T., Tkačik, G., Bialek, W., 2013. Statistical thermodynamics of natural images. Phys. Rev. Lett. 110, 018701. https://doi.org/10.1103/PhysRevLett.110.018701.
Stress: the health epidemic of the 21st century, SciTech connect. http://scitechconnect.elsevier.com/stress-health-epidemic-21st-century/, 2016–. (Accessed 27 May 2017).
Teghtsoonian, R., 1975. Psychophysics: Introduction to its Perceptual, Neural, and Social Prospects.
Tolhurst, D.J., Tadmor, Y., Chao, T., 1992. Amplitude spectra of natural images. Ophthalmic Physiol. Opt. 12, 229–232. https://doi.org/10.1111/j.1475-1313.1992.tb00296.x.
Towers, D.N., Allen, J.J.B., 2009. A better estimate of the internal consistency reliability of frontal EEG asymmetry scores. Psychophysiology 46, 132–142. https://doi.org/10.1111/j.1469-8986.2008.00759.x.
Ulrich, R.S., Zimring, C., Zhu, X., DuBose, J., Seo, H.-B., Choi, Y.-S., Quan, X., Joseph, A., 2008. A review of the research literature on evidence-based healthcare design. HERD 1, 61–125. https://doi.org/10.1177/193758670800100306.
Wang, C., Zhang, F., Wang, J., Doyle, J.K., Hancock, P.A., Mak, C.M., Liu, S., 2021. How indoor environmental quality affects occupants' cognitive functions: a systematic review. Build. Environ. 193, 107647. https://doi.org/10.1016/j.buildenv.2021.107647.
Wilkins, A., 2016. A physiological basis for visual discomfort: application in lighting design. Light. Res. Technol. 48, 44–54. https://doi.org/10.1177/1477153515612526.
Williams, N.S., McArthur, G.M., De Wit, B., Ibrahim, G., Badcock, N.A., 2020. A validation of Emotiv EPOC flex saline for EEG and ERP research. PeerJ 8, e9713. https://doi.org/10.7717/peerj.9713.
Wu, Q., Li, N., Cai, X., He, Y., Du, Y., 2023. Impact of indoor environmental quality (IEQ) factors on occupants' environmental perception and satisfaction in hospital wards. Build. Environ. 245, 110918. https://doi.org/10.1016/j.buildenv.2023.110918.
Zhang, S., Zheng, J., Wu, Y., 2020. Field study of air environment perceptions and influencing factors in waiting spaces of general hospitals in winter cities. Build. Environ. 183, 107203. https://doi.org/10.1016/j.buildenv.2020.107203.
Zhang, X., Hu, S., Guo, C., Liu, R., Tong, L., Shi, B., Li, B., 2023. Association between thermal comfort and cortisol depends on the air temperature and exposure time. Build. Environ. 233, 110073. https://doi.org/10.1016/j.buildenv.2023.110073.
Zhou, T., Wu, Y., Meng, Q., Kang, J., 2020. Influence of the acoustic environment in hospital wards on patient physiological and psychological indices. Front. Psychol. 11, 1600. https://doi.org/10.3389/fpsyg.2020.01600.